Biomedicine & Pharmacotherapy 198 (2026) 119220

Contents lists available at ScienceDirect

Biomedicine & Pharmacotherapy

journal homepage: www.elsevier.com/locate/biopha

Preclinical comparison of non-signaling domain in CD19 CAR T cell with interleukin-7 receptor alpha signaling domain

Pornlapat Keawvilai [a], Sirirut Jewmoung [a], Kristine Cate S. Pe [b], Supannikar Tawinwung [a,c,*], Koramit Suppipat [a,d,**]

[a] Center of Excellence in Cellular Immunotherapy, Chulalongkorn University, Bangkok, Thailand
[b] Department of Microbiology and Immunology, University of Otago, Dunedin, New Zealand
[c] Department of Pharmacology and Physiology, Faculty of Pharmaceutical Sciences, Chulalongkorn University, Bangkok, Thailand
[d] Department of Research Affairs, Faculty of Medicine, Chulalongkorn University, Bangkok, Thailand

ARTICLE INFO

Keywords:
B-cell malignancies
CD19
CAR T cell
IL-7 receptor alpha (IL-7Rα)
Non-signaling domain

ABSTRACT

Chimeric antigen receptor (CAR) T cells have emerged as an effective immunotherapy for hematologic malignancies. The non-signaling domain of CARs, comprising the spacer and transmembrane regions, is a key structural component that can be engineered to influence CAR expression and function. In this study, we evaluated three non-signaling domain configurations—IgG2.CH3/CD28, IgG2/CD28, and CD8/CD8—within a CD19 CAR construct incorporating 4–1BB and interleukin-7 receptor alpha (IL-7Rα) signaling domains. CARs incorporating the IgG2/CD28 domain exhibited reduced surface expression and diminished functional responses compared with IgG2.CH3/CD28 and CD8/CD8 constructs. The CD8/CD8 configuration supported the highest CAR expression and sustained surface density. In contrast, IgG2.CH3/CD28 CAR T cells displayed increased IL-2 and TNF-α secretion and enhanced CD107α upregulation following antigen stimulation. In a serial tumor cell rechallenge assay, IgG2.CH3/CD28 CAR T cells maintained cytotoxic activity and persistence compared with CD8/CD8 CAR T cells. In a NALM-6 xenograft model, IgG2.CH3/CD28 CAR T cells achieved durable tumor control and were associated with improved survival relative to CD8/CD8 CAR T cells. Collectively, these findings support the IgG2.CH3/CD28 non-signaling domain as a suitable structural component for CD19 CARs incorporating IL-7Rα signaling and provide insight into CAR design strategies aimed at improving T cell persistence and anti-leukemic activity.

1. Introduction

Adoptive cell transfer using T cells genetically engineered to express chimeric antigen receptors (CARs) has emerged as a transformative immunotherapy for hematologic malignancies. CAR T cells are designed to recognize tumor-associated antigens through synthetic receptors, enabling potent and antigen-specific cytotoxicity [1]. In particular, CD19-directed CAR T cell therapy has revolutionized the treatment of B-cell malignancies, leading to the regulatory approval of multiple products [2]. Despite these advances, a substantial proportion of patients experience relapse, often associated with limited CAR T cell persistence, T cell exhaustion, or antigen escape [3,4]. These challenges highlight the need for next-generation CAR designs with improved durability and functional fitness.

To overcome these limitations, advanced CAR engineering strategies have focused on augmenting the intrinsic fitness and persistence of T cells [5]. Our group previously established an IL-7Rα CAR platform by incorporating intracellular signaling interleukin-7 receptor alpha (IL-7Rα)—a key regulator of T cell homeostasis, survival, and memory differentiation—into the CAR signaling domain. This approach enhanced T cell proliferation, reduced activation-induced cell death, and improved anti-tumor activity in the context of B7-H3–targeted CAR T cells for solid tumors [6,7].

Beyond intracellular signaling domains, the non-signaling domain—comprising the spacer and transmembrane regions—plays a critical role in CAR performance. This structural component influences CAR surface expression, stability, immunological synapse formation, and antigen accessibility. Spacer length and composition can affect

* Correspondence to: Department of Pharmacology and Physiology, Faculty of Pharmaceutical Sciences, Chulalongkorn University, Bangkok 10330, Thailand.
** Correspondence to: Department of Research Affairs, Faculty of Medicine, Chulalongkorn University, Bangkok 10330, Thailand.
E-mail addresses: supannikar.t@pharm.chula.ac.th (S. Tawinwung), Koramit.s@chula.ac.th (K. Suppipat).

https://doi.org/10.1016/j.biopha.2026.119220
Received 20 January 2026; Received in revised form 6 March 2026; Accepted 11 March 2026
Available online 18 March 2026

epitope engagement, while the transmembrane domain may modulate receptor assembly and downstream signaling [8]. Optimization of the non-signaling domain can substantially impact CAR expression and cytotoxic function, highlighting that the optimal configuration is often context-dependent and requires validation for each CAR target [9,10].

In this study, we evaluated the impact of different non-signaling domains within a CAR construct incorporating IL-7Rα signaling in the context of CD19 targeting. We compared three distinct configurations: an IgG2.CH3 hinge/spacer with a CD28 transmembrane domain, an IgG2 hinge with a CD28 transmembrane domain, and a CD8 hinge/spacer with a CD8 transmembrane domain. We assessed how these structural variations influence CAR expression, functional activity, persistence, and anti-leukemic efficacy. This work aims to refine IL-7Rα–based CAR design and provide the development of effective CD19 CAR T cell therapies.

2. Materials and methods

2.1. Cell lines and cultures

B-cell acute lymphoblastic leukemia cell line NALM-6 (CRL-3273), Burkitt lymphoma cell line Raji (CCL-86), chronic myeloid leukemia cell line K562 (CCL-243), and human embryonic kidney cell line 293 T (CRL-3216) were purchased from the American Type Culture Collection (ATCC). Cells were cultured in either Roswell Park Memorial Institute (RPMI) 1640 Medium or Dulbecco's Modified Eagle Medium (DMEM) (Gibco, USA, Cat. No. 11965–092), supplemented with 10% fetal bovine serum (FBS) (Gibco, USA, Cat. No. 10270–106), 1% GlutaMax (Gibco, USA, Cat. No. 35050–061), and 1% penicillin-streptomycin (Gibco, USA, Cat. No. 15140–122). Cultures were incubated at 37 °C in a humidified atmosphere containing 5% CO_2. All cell lines were routinely screened using the MycoAlert™ Mycoplasma Detection Kit (Lonza) and were confirmed to be Mycoplasma-free prior to use in all experiments.

2.2. Isolation and activation of primary human T lymphocytes

Ethics approval for the use of primary cells was obtained from the Institutional Review Board, Faculty of Medicine, Chulalongkorn University (No. 0927/68). Peripheral blood mononuclear cells (PBMCs) were obtained from human blood samples using density gradient centrifugation with Ficoll-Paque™ Premium (Cytiva Cat. No. 17544202). T cells were activated in 24-well plates using T Cell TransAct™ (Miltenyi Cat. No. 130–128–758) in complete TexMACS medium (Miltenyi Biotec, Cat. No. 130–097–196) supplemented with 5% FBS, 10 ng/mL IL-7 (Miltenyi Biotec, Cat. No. 130–093–937), and 5 ng/mL IL-15 (Miltenyi Biotec, Cat. No. 130–095–762) prior to further experimental use.

2.3. Generation of CAR T cells

Lentiviruses were generated by co-transfecting 293 T cells with the plasmid encoding the CD19-CAR (CD19-specific scFv, FMC63) constructs, and the packaging plasmids (pMD2.G, pMDLg/pRRE, and pRSV) using GeneJuice® Transfection Reagent (Merckmillipore, Cat. No. 70967) according to the manufacturer's instructions. The lentiviral supernatants were collected at 48 and 72 h after transfection, filtered, and then mixed with Lenti-X Concentrator and incubated the mixture at 4°C for 30 min. The virus-containing pellet was collected by centrifuging at 1500 x g for 45 min at 4°C. Viral pellets were resuspended in TexMACS medium and aliquoted for long-term storage at −80 °C.

Primary activated T cells were transduced with lentivirus at a multiplicity of infection (MOI) of 3. CAR T cells were subsequently maintained by changing the culture media with TexMACS medium, supplemented with 10 ng/mL IL-7 (Miltenyi Biotec, Cat. No. 130–093–937) and 5 ng/mL IL-15 (Miltenyi Biotec, Cat. No. 130–095–762) every 3–4 days.

2.4. Flow cytometric staining

The antibodies utilized in this study were as follows: for CAR expression, PerCP/Cy5.5 anti-human CD3 (clone OKT3, Biolegend, USA, Cat. No. 317336) and PE-labeled monoclonal anti-FMC63 antibody (Cat. No. B73-H5253, Acro, USA). CAR T cell memory phenotype was identified by APC anti-human CD45RO (clone UCHL1, Biolegend, USA, Cat. No. 304210), FITC anti-human CCR7 (clone G043H7, Biolegend, USA, Cat. No. 353216). T cell subsets were identified by CD4-APC (clone OKT4, Biolegend, USA, Cat. No. 317416) and CD8-PE (clone SK1, Biolegend, USA, Cat. No. 344706). Activation markers were assessed by APC anti-human CD69 (clone FN50, Biolegend, USA, Cat. No. 310910) and PE anti-human CD25 (clone FN50, Cat. No. 302606, Biolegend, USA). Exhaustion marker expressions were investigated by FITC anti-human PD-1 (clone EH12.2H7, Cat. No. 329904, Biolegend, USA), PE anti-human TIGIT (clone A15153G, Biolegend, USA, Cat. No. 372704), APC anti-human TIM-3 (clone F38–2E2, Biolegend, USA, Cat. No. 345012), and PE anti-human LAG-3 (clone 11C3C65, Biolegend, USA, Cat. No. 369306). Cell death was assessed by Annexin V staining (Biolegend, USA, Cat. No. 640914). Flow cytometry was performed using a BD Accuri™ C6 Plus flow cytometer (BD Biosciences, USA), and the data were analyzed using FlowJo software v.10 (TreeStar, USA). Gating strategies were illustrated in Supplementary Fig S1–2.

2.5. Cytotoxicity assay

NALM-6 and K562 cells (target cells) were co-cultured with effector cells at 1:1, 1:2, and 1:4 (E:T ratio) for 24 h. For Raji cell line, target cells were co-cultured with effector cells at 4:1, 2:1, and 1:1 for 24 h. The co-cultured cells were harvested and stained with 7-AAD dye (BD Pharmingen™ Cat. No. 51–68981E) to exclude dead cells and APC anti-human CD3 (clone OKT3, Biolegend, USA, Cat. No. 317318) to identify effector cells. Viable target and effector cell counts were determined using an Accuri C6 flow cytometer with a fixed acquisition volume. Specific lysis was calculated using the following formula:

Specific lysis (%) = 100 - ((N target cell after co-culture / N target cell in target alone) x 100)

2.6. Cytokine analysis

The effector cells were co-cultured with tumor cells at a 1:1 ratio without the addition of exogenous cytokines. The supernatant was collected after co-culturing for 24 h. Secreted cytokines were assessed using a BD cytometric bead array (CBA)(BD Biosciences, USA) according to the manufacturer's instructions.

2.7. Tumor cell rechallenge assay

Non-transduced and CAR T cells (1×10^6 cells/well) were co-cultured with GFP^+ NALM-6 or Raji cells (1×10^6 cells/well) in TexMACS medium containing 5% FBS at an E:T ratio of 1:1 using 24-well G-rex plates (Wilson Wolf, Saint Paul, Minnesota, United States), without exogenous cytokines. Every four days, T cells were harvested, assessed with tumor cells by flow cytometry, and re-exposed to fresh target cells at the initial ratio. CAR T cell function was assessed by quantifying live cells with negative 7-AAD of GFP^+ tumor cells and $CD3^+$ T cells. The absolute number of residual effector cells was subsequently determined by multiplying the total viable cell count by the percentage of CD3 + identified through flow cytometric analysis at each rechallenge interval. The T cell functions were analyzed with exhaustion markers (PD-1, TIGIT, LAG3, TIM3) and memory phenotypes (CD45RO, CCR7).

2.8. Xenograft mouse models

The animal procedures were reviewed and approved by the Chulalongkorn University Animal Care and Use Committee, protocol No.

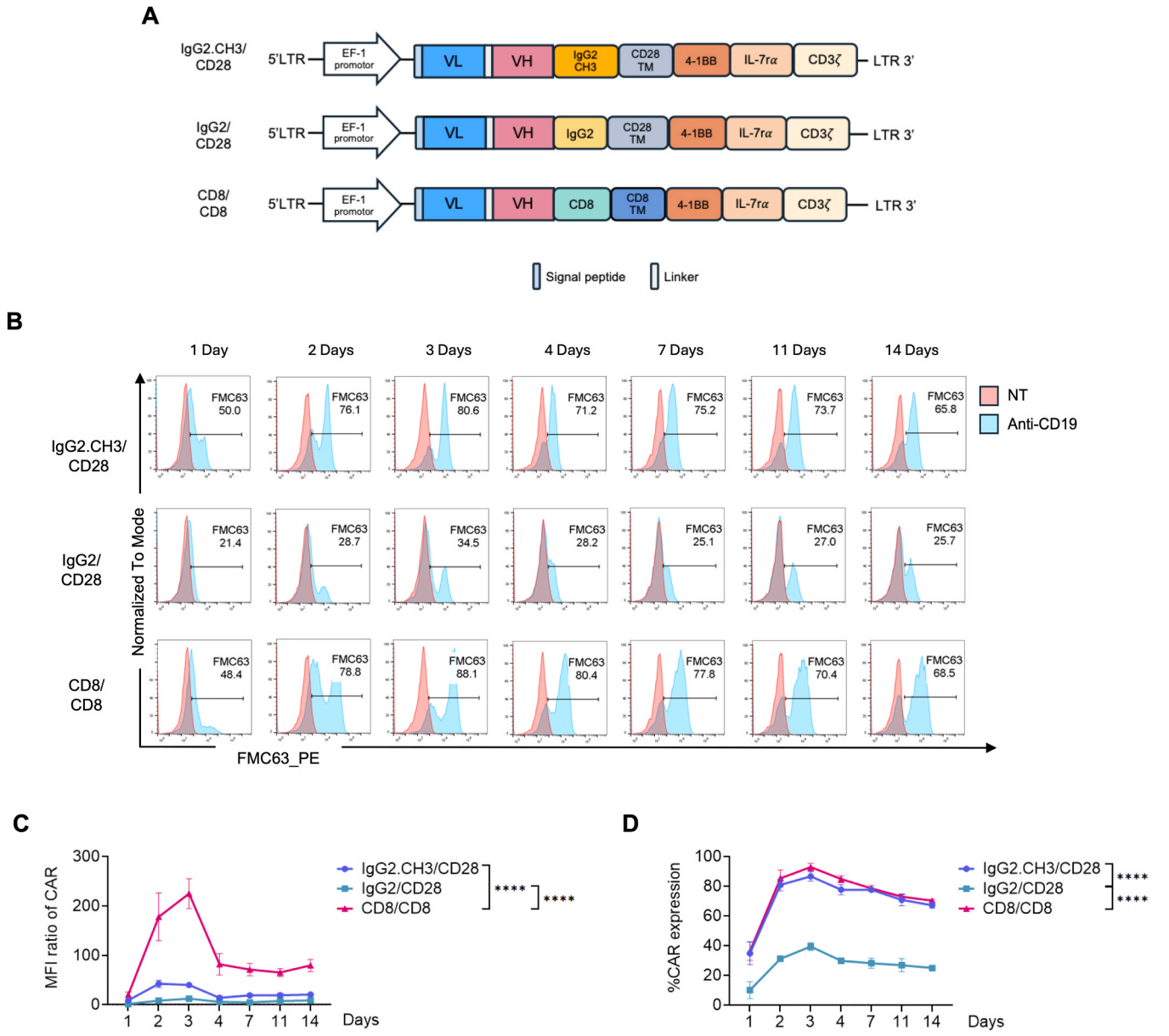

Fig. 1. Design and kinetic expression of CD19 IL-7Rα CAR constructs with different non-signaling domains. (A) Schematic representation of the CD19 IL-7Rα CAR constructs. Each construct contains an anti-FMC63 scFv, a non-signaling domain (IgG2.CH3, IgG2, or CD8α), a transmembrane domain (CD28 or CD8α), a 4–1BB, an IL-7Rα, and a CD3ζ cytoplasmic domain. (B) Representative flow cytometry histograms showing CAR expression on transduced T cells at days 1, 2, 3, 4, 7, 11, and 14 post-transduction. Non-transduced (NT) T cells are shown in red, and CD19 IL-7Rα CAR T cells are shown in blue. (C-D) Quantification of CAR expression kinetics. The percentage of CAR-positive T cells (C) and the mean fluorescence intensity (MFI) (D) were monitored over 14 days. Data are represented as mean ± SEM from three independent donors (n = 3). Statistical significance was determined by two-way ANOVA with Tukey's multiple comparisons test (****$p < 0.0001$).

2473022. A total of 11 female NOD.Cg-Prkdcscid Il2rgtm1Wjl/SzJ (NSG) mice at 6–7 weeks of age were engrafted intravenously (i.v.) with 0.25 × 106 NALM-6 cells. Following tumor establishment, mice were randomly assigned to three experimental groups (NT, n = 3; IgG2.CH3/CD28, n = 4; CD8/CD8, n = 4) based on baseline the bioluminescence imaging (BLI) signals to ensure balanced initial tumor burdens. Seven days post-engraftment, the mice were treated intravenously with 2 × 106 CAR T cells in PBS. Following CAR T cell infusion, tumor burden was monitored every 3–4 days using the IVIS Spectrum In Vivo Imaging System (PerkinElmer) and expressed as total flux (photons/s). Data analysis was performed using uniform Regions of Interest (ROI) settings across all groups to ensure objective quantification of the tumor burden. Body weight, CAR T cell persistence in peripheral blood, and the onset of GVHD were monitored weekly. All efforts were made to minimize animal suffering. Mice were humanely sacrificed when the 20% of body weight loss or showed signs of discomfort.

2.9. Statistical analysis

All statistical tests were performed using GraphPad Prism software v.7, which was used to analyze and visualize the results. One-way or two-way ANOVA followed by Tukey's multiple comparison test was performed to assess differences between groups or between each group and the indicated control. Survival determined from the time of tumor cell injection was analyzed by the Kaplan-Meier method, and differences in survival between groups were compared by the Gehan-Breslow-Wilcoxon test. Data are presented as the mean ± SEM from at least three independent donors. *$p < 0.05$, ** $p < 0.01$, *** $p < 0.001$, **** $p < 0.0001$ as significant.

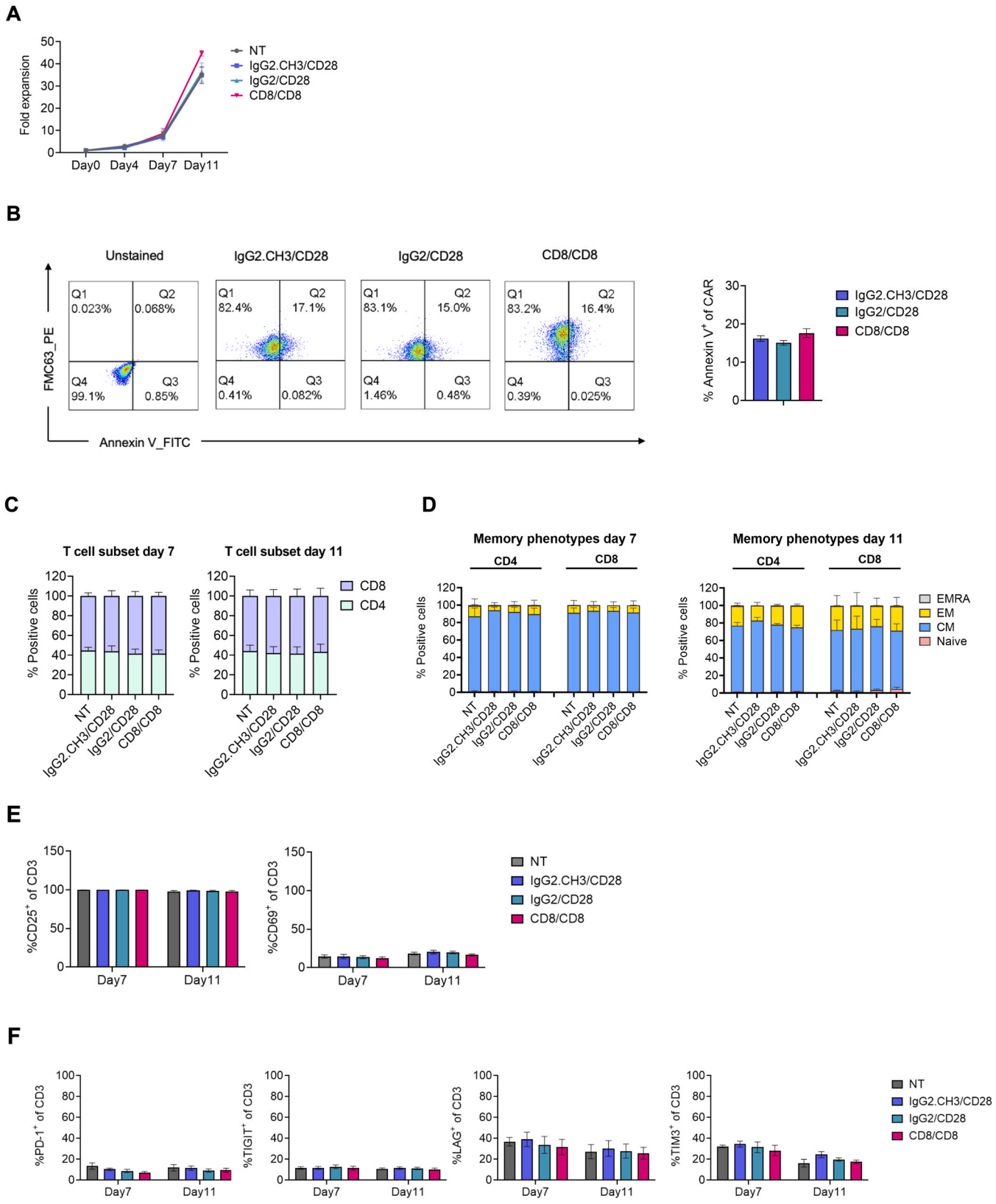

Fig. 2. CD19 IL-7Rα CAR T cells with different non-signaling domains show comparable expansion and phenotypes. (A) Proliferation of NT and CAR T cells was measured for 11 days post-transduction. (B) On day 7 post-transduction, CAR T cell apoptosis was evaluated using Annexin V staining. The percentage of Annexin V-positive cells within the CAR+ population was analyzed by flow cytometry. (C) Proportions of $CD4^+$ and $CD8^+$ T cells within the CD3 + populations at days 7 and 11. (D) Memory phenotypes of $CD4^+$ and $CD8^+$ T cells at days 7 and 11, defined by CD45RO and CCR7 expression: Naïve ($CD45RO^-CCR7^+$), Central Memory (CM, $CD45RO^+CCR7^+$), Effector Memory (EM, $CD45RO^+CCR7^-$), and Terminal Effector Memory RA (EMRA, $CD45RO^-CCR7^-$). (E-F) Expression of activation markers (CD25, CD69) (E) and exhaustion markers (PD-1, TIGIT, LAG3, TIM3) (F) on CD3 + cells at days 7 and 11. Data are represented as mean ± SEM from three independent donors (n = 3). Statistical significance was determined by one-way ANOVA with Tukey's multiple comparisons test.

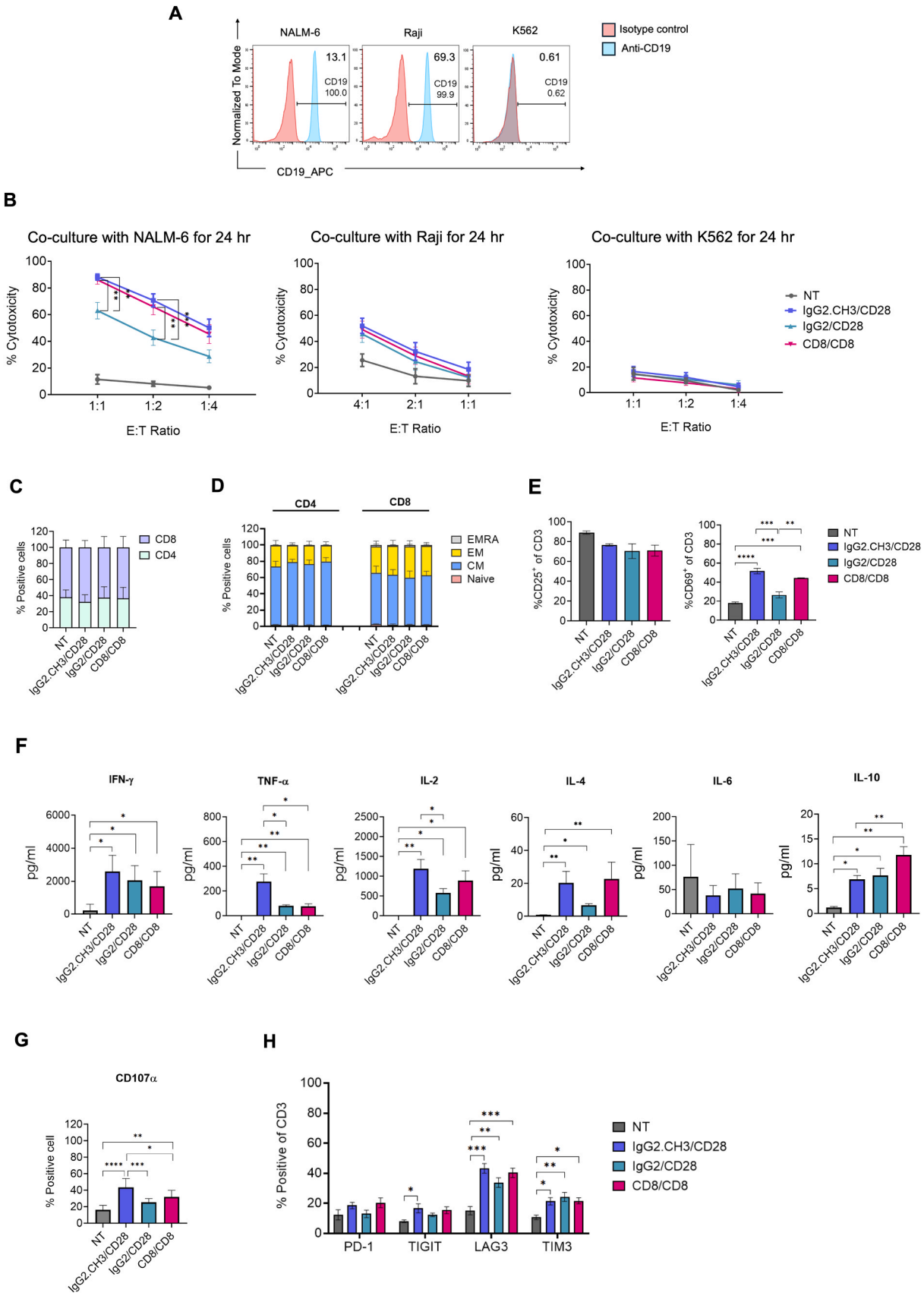

(caption on next page)

Fig. 3. In vitro anti-tumor functionality of anti-CD19 CAR T cells. (A) CD19 expression on target cell lines NALM-6, Raji, and the CD19-negative control cell line K562. (B) Cytotoxicity of CAR T cells co-cultured with NALM-6, Raji or K562 cells for 24 h at indicated Effector:Target (E:T) ratios. Data are represented as mean ± SEM from three independent donors (n = 3). Statistical significances were determined by one-way ANOVA (** $p < 0.01$, *** $p < 0.001$). (C) Proportions of $CD4^+$ and $CD8^+$ T cells after a 24-hour co-culture with NALM-6 cells. (D) Memory phenotypes of $CD4^+$ and $CD8^+$ T cells after co-culture. (E) Expression of the activation marker CD25 and CD69 on T cells after co-culture. Data are represented as mean ± SEM from three independent donors (n = 3). Statistical significances were determined by one-way ANOVA with Tukey's multiple comparisons test. (** $p < 0.01$, *** $p < 0.001$, **** $p < 0.0001$). (F) Cytokine concentrations in supernatants from 24-hour co-culture with NALM-6 cells. Data are represented as mean ± SEM from three independent donors (n = 3). Statistical significances were determined by one-way ANOVA with Tukey's multiple comparisons test. (*$p < 0.05$, **$p < 0.01$). (G) Degranulation of CAR T cells, measured by surface CD107α expression, after co-culture. Data are represented as mean ± SEM from seven independent donors (n = 7). Statistical significances were determined by one-way ANOVA with Tukey's multiple comparisons test. (* $p < 0.05$, ** $p < 0.01$, *** $p < 0.001$, **** $p < 0.0001$). (H) Expression of the exhaustion marker on T cells after co-culture. Data are represented as mean ± SEM from three independent donors (n = 3). Statistical significances were determined by one-way ANOVA with Tukey's multiple comparisons test. (* $p < 0.05$, ** $p < 0.01$, *** $p < 0.001$).

3. Results

3.1. CD8/CD8 non-signaling domain enhances CAR expression density in CD19 IL-7Rα CAR T cells

CAR T cells incorporating the 4–1BB and IL-7Rα signaling domains (41BB-IL-7Rα) were previously developed by our group and demonstrated superior functionality in targeting the solid tumor antigen B7H3 [6]. In this study, we aimed to characterize the effect of different non-signaling domains on CD19 CAR T cells engineered with an IL-7Rα endodomain. Three commonly used non-signaling hinge/spacer domains were evaluated. We engineered anti-CD19 CARs containing one of the following designs: an IgG2.CH3 spacer with a CD28 transmembrane (TM) domain (IgG2.CH3/CD28), an IgG2 spacer with a CD28 TM domain (IgG2/CD28), or a CD8 spacer with a CD8 TM domain (CD8/CD8) (Fig. 1A). To ensure equivalent exposure to viral particles, T cells were transduced at a multiplicity of infection (MOI) of 3. CAR expression kinetics were then monitored from day 1 to day 14 post-transduction (Fig. 1B). The IgG2/CD28 construct yielded significantly lower CAR expression measured by both the percentage of CAR^+ cells and mean fluorescence intensity (MFI) compared with the IgG2.CH3/CD28 and CD8/CD8 constructs (Fig. 1C–D). While both IgG2.CH3/CD28 and CD8/CD8 constructs produced a high proportion of CAR^+ T cells, the CD8/CD8 construct exhibited significantly higher peak and sustained MFI than IgG2.CH3/CD28. To determine whether differences in CAR expression across non-signaling domains were specific to the CD19 CAR context, we generated anti-B7H3/IL-7Rα CAR T cells using the same three non-signaling domains. Consistently, the IgG2/CD28 construct showed the lowest CAR expression compared with the other two designs (Supplementary Fig S3A–C), whereas IgG2.CH3/CD28 and CD8/CD8 resulted in comparable percentages of CAR^+ cells and MFI. These results suggest that the CD8/CD8 and IgG2.CH3/CD28 non-signaling domains yield high CAR expression in CD19 CAR T cells incorporating the IL-7Rα signaling domain.

3.2. CD19 IL-7Rα CAR T cells with different non-signaling domains show comparable expansion and phenotypes

High CAR surface expression can lead to ligand-independent clustering and tonic signaling, potentially driving T cell exhaustion [11]. We therefore investigated whether the differential CAR expression levels observed across non-signaling domains were associated with changes in T cell proliferation, apoptosis, or phenotype following transduction. We observed comparable T cell expansion between CD19 IL-7Rα CAR T cells containing the IgG2/CD28 and IgG2.CH3/CD28 constructs, whereas CAR T cells incorporating the CD8/CD8 domain exhibited a modest increase in expansion at day 11 post-transduction; however, this difference did not reach statistical significance (Fig. 2A). This increase was not accompanied by elevated apoptosis, as the frequency of Annexin V^+ cells at day 7 was similar across all constructs (Fig. 2B). We next compared T cell phenotypes among the three constructs at days 7 and 11 post-transduction. The proportions of $CD4^+$ and $CD8^+$ T cells were comparable between groups (Fig. 2C). For memory subset analysis, CD45RO and CCR7 expression within $CD4^+$ and $CD8^+$ T cell populations was used to define naïve ($CD45RO^-CCR7^+$), central memory (CM; $CD45RO^+CCR7^+$), effector memory (EM; $CD45RO^+CCR7^-$), and terminally differentiated effector (EMRA; $CD45RO^-CCR7^-$) subsets. Both $CD4^+$ T cells and $CD8^+$ T cells showed similar distributions of CD45RO and CCR7 expression across constructs (Fig. 2D). Furthermore, the expression of activation markers (CD25, CD69) and exhaustion markers (PD-1, TIGIT, LAG-3, TIM-3) was comparable among all three CAR designs (Fig. 2E–F). Collectively, these results indicate that the higher surface CAR density observed with the CD8/CD8-based CD19 CAR does not significantly alter the baseline phenotype of the resulting CAR T cells.

3.3. IgG2.CH3/CD28 and CD8/CD8 CD19 IL-7Rα CAR T cells exhibit potent in vitro efficacy against $CD19^+$ cell lines

To evaluate the effect of the non-signaling domain on the antigen-specific activity of anti-CD19 IL-7Rα CARs, we co-cultured CAR T cells with CD19-positive cell lines (NALM-6 and Raji) and a CD19-negative cell line (K562) (Fig. 3A). Co-cultures were performed for 24 h at various effector-to-target ratios: 1:1, 1:2, and 1:4 for NALM-6 and K562, and 4:1, 2:1, and 1:1 for Raji. These ratios were established based on our preliminary optimization, which indicated that Raji cells require a higher effector-to-target ratio in in vitro culture than NALM-6 cells. Non-transduced T cells (NT) served as negative controls. All CD19 IL-7Rα CAR T cells incorporate IgG2.CH3/CD28, IgG2/CD28, and CD8/CD8 non-signaling domains mediated antigen-specific lysis of CD19 + cell lines in a dose-dependent manner, while exhibiting no cytotoxicity toward CD19-negative K562 cells, thereby confirming target specificity (Fig. 3B). Notably, IgG2/CD28 CAR T cells demonstrated significantly reduced cytotoxicity against NALM-6 cells for 24 h compared with IgG2.CH3/CD28 and CD8/CD8, consistent with their lower CAR surface expression.

T cell subset and memory phenotypes following co-culture with NALM-6 were then analyzed. The proportions of $CD4^+$ and $CD8^+$ T cell subsets did not differ significantly among constructs (Fig. 3C). Memory phenotypes of CD19 IL-7Rα CAR T cells after antigen stimulation were also comparable across the different hinge/spacer domains (Fig. 3D). To examine activation status, we evaluated CD25 and CD69 expression following antigen stimulation. CD25 expression remained comparable among all constructs. In contrast, IgG2.CH3/CD28 and CD8/CD8 CAR T cells displayed significantly higher CD69 expression than IgG2/CD28, aligning with their enhanced cytotoxic activity (Fig. 3E). Supernatants collected after 24 h of co-culture with NALM-6 were analyzed for cytokine secretion. All CD19 IL-7Rα CAR T cells produced higher cytokine levels compared with NT controls. Among the constructs, IgG2.CH3/CD28 exhibited significantly higher levels of IFN-γ, TNF-α, and IL-2 than the other non-signaling domains, whereas the CD8/CD8 CAR T cells secreted higher levels of the regulatory cytokine IL-10. No statistically significant differences in IL-4 and IL-6 levels were observed among the three constructs (Fig. 3F).

We next evaluated CD107α expression, an indicator of T cell degranulation, following stimulation with NALM-6 cells for 4 h. IgG2.CH3/CD28 CAR T cells exhibited the highest CD107α expression levels,

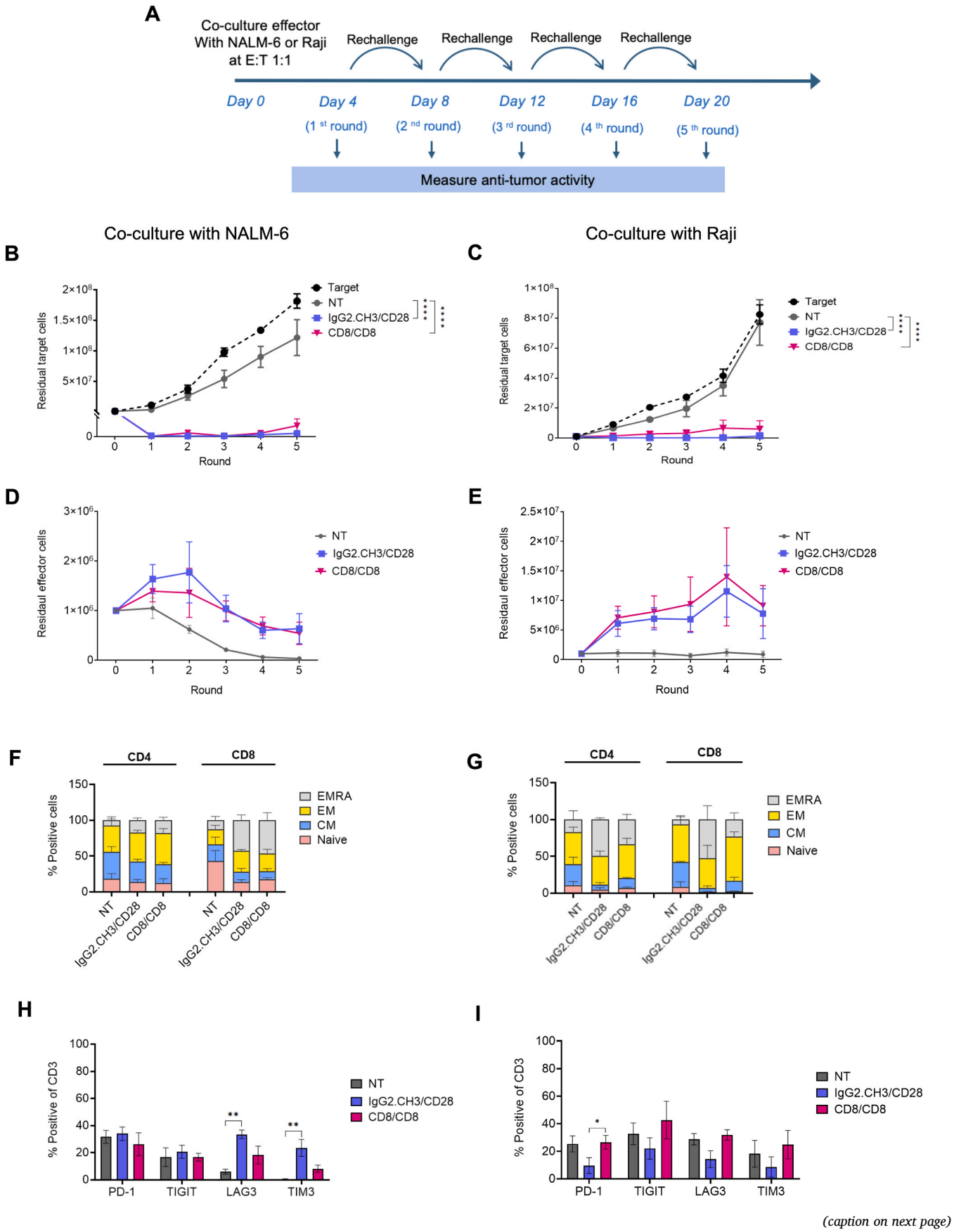

(caption on next page)

Fig. 4. CD19 IL-7Rα CAR T cells maintain sustained effector activity during repeated tumor cell rechallenge in vitro. (A) Schematic of the in vitro tumor cell rechallenge assay. CAR T cells were co-cultured with NALM-6 or Raji-GFP target cells at 1:1 (E:T) ratio and restimulated with tumor cells every 4 days for five rounds. (B-C) Absolute numbers of residual target tumor cells quantified at each round of NALM-6 (B) and Raji-GFP (C) co-cultures, reflecting sustained cytotoxic activity of CAR T cells upon repeated antigen exposure. (D-E) Absolute numbers of effector CAR T cells measured throughout the tumor cell rechallenge assay in NALM-6 (D) and Raji-GFP (E) co-cultures, indicating CAR T cell expansion and persistence during chronic antigen stimulation. Data are represented as mean ± SEM from three independent donors (n = 3). Statistical significance was determined by two-way ANOVA with Tukey's multiple comparisons test (****$p < 0.0001$). (F-G) Analysis of T cell phenotypes at the third round of rechallenge with NALM-6 (F) or Raji (G) cells. (H-I) Exhaustion marker expression was assessed at the third round of rechallenge with NALM-6 (H) or Raji (I) cells. Data are represented as mean ± SEM from three independent donors (n = 3). Statistical significance was determined by one-way ANOVA with Tukey's multiple comparisons test. (* $p < 0.05$, ** $p < 0.01$).

CD8/CD8 showed intermediate levels, and IgG2/CD28 displayed the lowest expression (Fig. 3G). The reduced CD107α expression observed in IgG2/CD28 CAR T cells was consistent with their diminished cytotoxic function. Finally, we assessed exhaustion markers expression after antigen stimulation. No significant differences in PD1, TIGIT, LAG3, and TIM3 expression were observed among all three constructs, although LAG3 and TIM3 were upregulated in all CAR T groups compared with NT (Fig. 3H).

3.4. CD19 IL-7Rα-CAR T cells incorporating IgG2.CH3/CD28 demonstrated reduced exhaustion markers in an in vitro tumor cell rechallenge assay

The IgG2/CD28 non-signaling domain demonstrates inferior CAR expression and reduced cytotoxic functions compared with the other non-signaling domains. Therefore, the subsequent comparative analysis was restricted to the IgG2.CH3/CD28 and CD8/CD8 domains to determine their tumor control and T cell persistence in a repetitive tumor cell rechallenge assay. CAR T cells were co-cultured with GFP-expressing NALM-6 or Raji cells at 1:1 E:T ratio, and their cytotoxicity and T cell persistence were assessed across five rounds of rechallenge with fresh tumor cells every 4 days (Fig. 4A). After rechallenge with NALM-6 or Raji cells, the CD19 IL-7Rα CAR T cells incorporated IgG2.CH3/CD28 and CD8/CD8 non-signaling domains effectively eliminated NALM-6 and Raji cells (Fig. 4B-C). Both CAR T cell constructs expanded robustly compared with non-transduced (NT) T cells, with no significant differences in T cell persistence between the two CAR designs (Fig. 4D–E). After the third round of co-culture, both CAR T cell groups exhibited a more differentiated phenotype compared with NT controls, characterized by increased effector memory and EMRA populations, with no significant differences between IgG2.CH3/CD28 and CD8/CD8 constructs in either target model (Fig. 4F–G). Exhaustion marker analysis following the third round of co-culture showed target-dependent differences. In the NALM-6 model, IgG2.CH3/CD28 CAR T cells showed higher LAG-3 and TIM-3 expression, whereas in the Raji model, CD8/CD8 CAR T cells exhibited higher PD-1 expression compared with IgG2.CH3/CD28 (Fig. 4H–I).

3.5. CD19 IL-7Rα CARs incorporating IgG2.CH3/CD28 suppresses tumor burden and improves survival in a NALM-6 xenograft model

To investigate the therapeutic potential of CD19 IL-7Rα CARs incorporating either IgG2.CH3/CD28 or CD8/CD8 non-signaling domains, we employed a systemic NALM-6 xenograft model using NSG mice. Mice were intravenously engrafted with 2.5×10^5 NALM-6-Luc cells, followed by intravenous administration of 2.0×10^6 CAR T cells seven days later (Fig. 5A). Tumor burden was monitored weekly by bioluminescent imaging (BLI), and CAR T cell persistence in peripheral blood was assessed by flow cytometric analysis of $CD45^+CD3^+$ populations. CD19 IL-7Rα CAR T cells incorporating IgG2.CH3/CD28 domain demonstrated markedly superior anti-tumor activity compared with those incorporating the CD8/CD8 domain, as evidenced by a significant reduction in tumor-derived bioluminescence signals over time (Fig. 5B-D). Consistent with enhanced tumor control, mice were treated with IgG2.CH3/CD28 CD19 IL-7Rα CAR T cells exhibited significantly prolonged survival relative to the CD8/CD8 CAR T cell group (Fig. 5E). No significant differences in body weight were observed among experimental groups (Fig. 5F). Notably, peripheral blood analysis revealed significantly higher levels of circulating $CD45^+CD3^+$ CAR T cells at day 28 in mice receiving IgG2.CH3/CD28 CAR T cells, suggesting enhanced in vivo persistence and/or proliferation (Fig. 5G). Collectively, these results demonstrate that incorporating IgG2.CH3/CD28 non-signaling domain provides favorable anti-tumor responses in the context of CD19 CARs containing IL-7Rα.

4. Discussion

In this study, we optimized the non-signaling domain in CD19 IL-7Rα CARs by comparing three common non-signaling domains with 4–1BB-IL-7Rα-CD3ζ signaling domains. Previous studies have demonstrated that the incorporation of IL-7Rα together with an IgG2.CH3/CD28 hinge/spacer enhances CAR T cell persistence and therapeutic efficacy in B7H3-directed CAR T cells for glioblastoma [6]. Consistent with these findings, we observed that CD19 IL-7Rα CARs with the IgG2.CH3/CD28 non-signaling domain outperformed those containing IgG2/CD28 or CD8/CD8 domains, exhibiting stronger antigen-dependent activation and enhanced cytokine secretion in vitro. Moreover, IgG2.CH3/CD28 CAR T cells effectively eradicated tumors and significantly prolonged survival in vivo compared with CAR T cells incorporating the CD8/CD8 domain. These data highlight the non-signaling domain as a critical yet often underappreciated determinant of CAR T-cell potency.

Previous studies have extensively explored CAR structural optimization to enhance T cell efficacy and persistence [2,12–15]. Among CAR components, the spacer/hinge and transmembrane (TM) regions, collectively referred to as the non-signaling domain, play critical roles in modulating CAR expression, stability, and functional activity [13]. To examine the contribution of these elements, we evaluated CAR constructs incorporating spacer/hinge/TM domains of varying length and composition, including a long IgG2.CH3/CD28 spacer (148 amino acids), an intermediate CD8/CD8 spacer (69 amino acids), and a short IgG2/CD28 spacer (39 amino acids). Our data indicate that the short IgG2/CD28 non-signaling domain resulted in poor CAR surface expression, leading to impaired CAR T cell function. These findings are consistent with previous reports demonstrating that spacer length is a critical determinant of CAR expression, with full-length spacers supporting higher surface expression compared with shortened constructs [13]. In addition to spacer length, the structural composition of the non-signaling domain is a key factor influencing proper protein folding, stability, and trafficking of the CAR to the cell surface [13]. The IgG2 constant heavy chain 3 (CH3) domain was therefore selected to provide sufficient spacer length while minimizing off-target Fcγ receptor interactions that have been associated with full IgG-Fc spacers containing both CH2 and CH3 domains [16–18].

Our results demonstrate that the CAR construct containing the CD8 spacer and CD8 transmembrane (CD8/CD8) domains exhibited significantly higher and more sustained surface expression compared to the IgG2.CH3/CD28 construct. This is consistent with previous studies demonstrating superior CAR expression and stability in the CD8/CD8-based anti-TIM3 CAR and GXMR-CAR [9,19]. Moreover, prior work has suggested that the transmembrane domain can be the primary determinant of surface expression levels rather than the spacer domain in mVEGFR2-specific CARs [12]. Despite exhibiting lower CAR surface

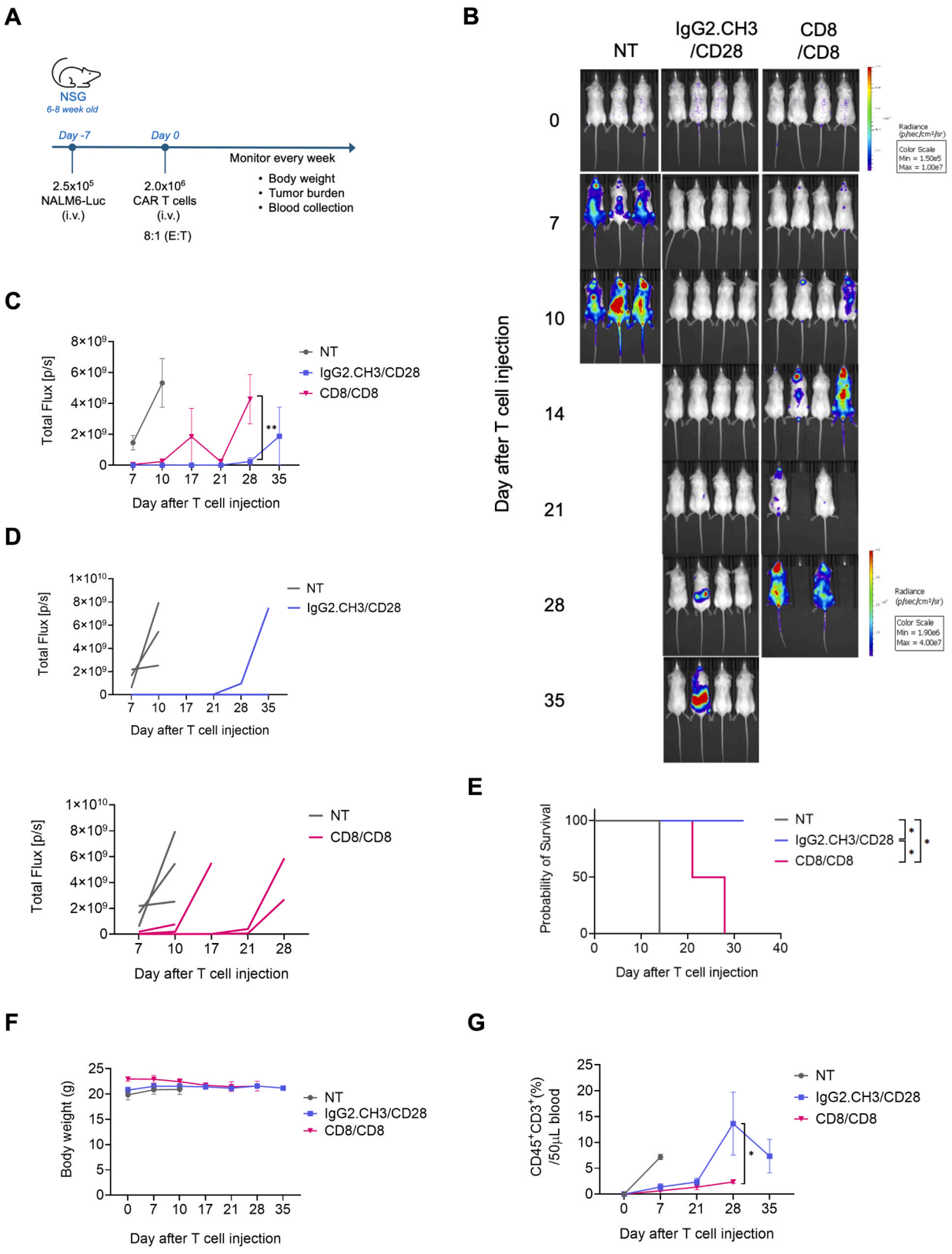

Fig. 5. The IgG2.CH3/CD28 CAR construct demonstrates superior anti-tumor efficacy in a NALM-6 xenograft model. (A) Schematic of the in vivo study, NSG mice were injected intravenously (i.v.) with 2.5×10^5 NALM-6-Luc cells, followed by i.v. injection of 2.0×10^6 NT or CAR T cells 7 days later. (B) Representative bioluminescence imaging (BLI) of tumor burden in mice from each group at the indicated time points. (C-D) Quantification of tumor burden shown as total flux from individual mice (C) and as the group average (D). Data are represented as mean ± SEM, (n = 3–4). Statistical significance was determined by two-way ANOVA with Tukey's multiple comparisons test (** $p < 0.01$). (E) Kaplan-Meier survival analysis of mice in each treatment group, Gehan- Breslow- Wilcoxon test (* $p < 0.05$), (n = 3–4). (F) Mouse body weight was monitored weekly. (G) Absolute counts of circulating human T cells ($CD45^+CD3^+$) in peripheral blood. Data are represented as mean ± SEM, (n = 3–4). Statistical significance was determined by two-way ANOVA with Tukey's multiple comparisons test (*$p < 0.05$).

expression (MFI), the CD19 IL-7Rα CAR T cells incorporating the IgG2.CH3/CD28 non-signaling domain demonstrated higher CD69 expression, enhanced degranulation, and increased IFN-γ, TNF-α, and IL-2 secretion compared with the CD8/CD8 construct following antigen exposure. A previous study by Alabanza et al. also showed that, in CARs containing CD28 co-stimulatory domains, constructs with CD28 hinge/transmembrane regions resulted in higher cytokine secretion and degranulation compared with similar CARs containing the CD8α hinge/transmembrane domains [20]. In addition, the CD28 transmembrane has been previously shown to heterodimerize with endogenous CD28, an interaction that enhances downstream signaling, including IFN-γ production [14]. However, whether heterodimerization between the CD28 transmembrane domain in the CAR construct and endogenous CD28 contributes to the enhanced effector function observed in our IgG2.CH3/CD28 construct remains unclear. Future mechanistic investigation, such as co-immunoprecipitation or knockdown of endogenous CD28, would be required to address this possibility.

In the present study, we observed differences in CAR T-cell killing kinetics between the two CD19⁺ target cell lines used. Under co-culture conditions at an E:T ratio of 1:1 for 24 h, cytotoxicity against NALM-6 cells reached approximately 80–90%, whereas cytotoxicity against Raji cells remained below 30%. This observation suggests that Raji cells require higher E to T ratios to achieve comparable levels of tumor cell killing and exhibit more resistance to CAR T cell–mediated cytotoxicity. Such variability may reflect intrinsic differences between cancer cell types, including antigen density, growth characteristics, or resistance to immune-mediated killing [4,21]. In addition, our in vitro assays were performed using established cell lines rather than primary patient-derived samples. While commonly used cell line models enable controlled comparison of CAR constructs, they do not fully capture the biological heterogeneity of primary B-cell malignancies. Nevertheless, the anti-tumor activity observed in vitro was supported by the NALM-6 xenograft model in vivo, which confirmed the results observed in vitro.

Under chronic antigen exposure, IgG2.CH3/CD28 CAR T cells exhibited cytotoxic activity to NALM-6 cells, although this sustained activity was accompanied by increased LAG3 and TIM3 expression. These markers likely reflect persistent activation or a production exhaustion state rather than terminal dysfunction [22–24]. In contrast, Raji's rechallenge revealed a target-dependent divergence in exhaustion profiles. The IgG2.CH3/CD28 CAR exhibited significantly lower PD-1 expression than the less effective CD8/CD8 CAR. This tumor-derived exhaustion may reflect the higher CD19 antigen density in Raji or additional immune mediators between NALM-6 and Raji cells [25–27]. In addition to exhaustion status, metabolic profiling—specifically oxygen consumption rate (OCR) and extracellular acidification rate (ECAR)—has also been shown to serve as an indicator of T-cell persistence by distinguishing long-lived memory subsets from exhaustion-prone effector cells within the tumor microenvironment [28–30].

The IgG2.CH3/CD28 CAR achieved tumor eradication and yielded longer survival in the NALM-6 xenograft model compared with the CD8/CD8 CAR. Circulating CAR⁺ cells were also detected at higher levels in mice treated with IgG2.CH3/CD28 CAR T cells compared with the CD8/CD8 group, suggesting enhanced persistence of this construct. The increased systemic CAR⁺ cell levels correlated with the reduced tumor luminescence signal observed in mice receiving the IgG2.CH3/CD28 construct. However, quantification of CAR⁺ cells in the bone marrow or spleen was not performed in the present study, which could have provided additional evidence supporting the enhanced persistence of IgG2.CH3/CD28 CAR T cells. These in vivo findings are consistent with our in vitro results, in which IgG2.CH3/CD28 CAR T cells exhibited higher T-cell activation, degranulation, and Th1 cytokine production (IFN-γ, TNF-α, and IL-2).

Interestingly, we also observed elevated secretion of the regulatory cytokine IL-10 in CD8/CD8-based CAR T cells. The role of IL-10 in CAR T-cell function remains controversial. Recent studies suggest that IL-10 may alleviate T-cell exhaustion in cancer immunity through metabolic reprogramming [31,32], whereas previous studies have demonstrated that IL-10 neutralization can restore CAR T-cell activity [29]. Although the underlying mechanisms were not investigated in the context of our CAR constructs, our findings support a role for the non-signaling domain in shaping the antigen-induced cytokine response profile of CAR T cells, which may ultimately influence their anti-tumor capacity [16].

While our study provides a preclinical validation of an optimized CAR construct, limitations must be acknowledged. Although the immunodeficient NSG mouse models are standard for xenograft studies, they lacks a complete immune system. This environment cannot fully recapitulate the complex human tumor microenvironment, which includes suppressive myeloid cells and regulatory T cells [33]. In addition, this model does not allow evaluation of the potential effects of CAR T cells on endogenous bystander T cell activation, which has been reported to contribute to durable anti-tumor responses in immune-competent settings.

Our findings were primarily based on CD19 CAR constructs incorporating the widely used anti-CD19 scFv (FMC63). To assess whether the observed effects were specific to this antigen context, we performed parallel experiments using a B7-H3–targeted CAR construct. In this system, the IgG2/CD28 construct consistently exhibited lower CAR surface expression compared with the other two designs, whereas IgG2.CH3/CD28 and CD8/CD8 showed comparable percentages of CAR⁺ cells and MFI. These results suggest that the impact of the non-signaling domain may not be limited to a single antigen context. However, this observation should not be generalized to conclude that the IgG2.CH3/CD28 configuration would universally perform better across all target antigens or with other scFv clones. Previous study demonstrated that optimization of the transmembrane domain improved CAR internalization and recycling, thereby enhancing anti-tumor activity [34]. Although investigation of these mechanisms was beyond the scope of the current study, this represents an interesting direction for future work.

5. Conclusions

In summary, this study demonstrates that the non-signaling domain is a critical determinant of CAR T-cell performance in the context of an IL-7Rα–incorporated CD19 CAR platform. Among the designs tested, the IgG2.CH3/CD28 non-signaling domain supported favorable CAR expression, effector function, and persistence. Despite lower surface CAR density compared with CD8/CD8, IgG2.CH3/CD28 CAR T cells showed stronger antigen-dependent activation, sustained cytotoxicity during repeated tumor exposure, and improved tumor control and survival in vivo. These findings support the IgG2.CH3/CD28–4–1BB-IL-7Rαζ configuration as a suitable design for CD19 CAR T cells.

CRediT authorship contribution statement

Koramit Suppipat: Writing – review & editing, Supervision, Funding acquisition, Conceptualization. **Pornlapat Keawvilai:** Writing – original draft, Visualization, Investigation, Formal analysis, Data curation. **Sirirut Jewmoung:** Investigation, Formal analysis. **Kristine Cate S. Pe:** Methodology, Investigation. **Supannikar Tawinwung:** Writing – review & editing, Supervision, Funding acquisition, Conceptualization.

Declaration of Competing Interest

The authors declare that there are no conflicts of interest.

Acknowledgments

This research project is supported by the Ratchadapisek Somphot Fund for Postdoctoral Fellowship, Chulalongkorn University, the Thailand Science Research and Innovation Fund Chulalongkorn University (HEA_FF_69_231_3000_032), National Research Council of

Thailand (NRCT) and Chulalongkorn University (N42A680237). The academic endeavors of Thailand Hub of Talents in Cancer Immunotherapy (TTCI) receive support from the National Research Council of Thailand.

Appendix A. Supporting information

Supplementary data associated with this article can be found in the online version at doi:10.1016/j.biopha.2026.119220.

Data availability

Data will be made available on request.

References

[1] B.C. Miller, M.V. Maus, CD19-Targeted CAR T Cells: A New Tool in the Fight against B Cell Malignancies, Oncol. Res Treat. 38 (12) (2015) 683–690, https://doi.org/10.1159/000442170.
[2] Y. Wang, Y.J. Xue, Y.X. Zuo, Y.P. Jia, A.D. Lu, H.M. Zeng, et al., CD19-Specific CAR-T Cell Treatment of 115 Children and Young Adults with Acute B Lymphoblastic Leukemia: Long-term Follow-up, Cancer Res Treat. 56 (3) (2024) 945–955, https://doi.org/10.4143/crt.2023.1205.
[3] N.N. Shah, T.J. Fry, Mechanisms of resistance to CAR T cell therapy, Nat. Rev. Clin. Oncol. 16 (6) (2019) 372–385, https://doi.org/10.1038/s41571-019-0184-6.
[4] R.G. Majzner, C.L. Mackall, Tumor Antigen Escape from CAR T-cell Therapy, Cancer Discov. 8 (10) (2018) 1219–1226, https://doi.org/10.1158/2159-8290.CD-18-0442.
[5] J. Li, G. Huston, S.L. Swain, IL-7 promotes the transition of CD4 effectors to persistent memory cells, J. Exp. Med 198 (12) (2003) 1807–1815, https://doi.org/10.1084/jem.20030725.
[6] N. Sakunrangsit, N. Khuisangeam, T. Inthanachai, V. Yodsurang, P. Taechawattananant, K. Suppipat, et al., Incorporating IL7 receptor alpha signaling in the endodomain of B7H3-targeting chimeric antigen receptor T cells mediates antitumor activity in glioblastoma, Cancer Immunol. Immunother. 73 (6) (2024) 98, https://doi.org/10.1007/s00262-024-03685-7.
[7] Y. Gong, W. Lin, X. Fang, R. Zhang, M. Luo, H. Wu, et al., Advances in Cellular Immune Theranostic Approaches for Glioblastoma: Current Trends and Future Directions, Cancer Innov. 4 (4) (2025) e70018, https://doi.org/10.1002/cai2.70018.
[8] R.D. Guest, R.E. Hawkins, N. Kirillova, E.J. Cheadle, J. Arnold, A. O'Neill, et al., The role of extracellular spacer regions in the optimal design of chimeric immune receptors: evaluation of four different scFvs and antigens, J. Immunother. 28 (3) (2005) 203–211, https://doi.org/10.1097/01.cji.0000161397.96582.59.
[9] K.C.S. Pe, S. Jewmoung, S.A.H. Rad, N. Chantarat, C. Chanswangphuwana, H. Tashiro, et al., Optimization of anti-TIM3 chimeric antigen receptor with CD8alpha spacer and TNFR-based costimulation for enhanced efficacy in AML therapy, Biomed. Pharm. 179 (2024) 117388, https://doi.org/10.1016/j.biopha.2024.117388.
[10] N. Wu, N. Yang, S. Zhang, H. Wu, X. Fang, W. Lin, et al., Chimeric antigen receptor NK cells for breast cancer immunotherapy, Cancer Treat. Rev. 137 (2025) 102943, https://doi.org/10.1016/j.ctrv.2025.102943.
[11] A.H. Long, W.M. Haso, J.F. Shern, K.M. Wanhainen, M. Murgai, M. Ingaramo, et al., 4-1BB costimulation ameliorates T cell exhaustion induced by tonic signaling of chimeric antigen receptors, Nat. Med 21 (6) (2015) 581–590, https://doi.org/10.1038/nm.3838.
[12] K. Fujiwara, A. Tsunei, H. Kusabuka, E. Ogaki, M. Tachibana, N. Okada, Hinge and Transmembrane Domains of Chimeric Antigen Receptor Regulate Receptor Expression and Signaling Threshold, Cells 9 (5) (2020), https://doi.org/10.3390/cells9051182.
[13] K. Fujiwara, M. Masutani, M. Tachibana, N. Okada, Impact of scFv structure in chimeric antigen receptor on receptor expression efficiency and antigen recognition properties, Biochem Biophys. Res Commun. 527 (2) (2020) 350–357, https://doi.org/10.1016/j.bbrc.2020.03.071.
[14] Y.D. Muller, D.P. Nguyen, L.M.R. Ferreira, P. Ho, C. Raffin, R.V.B. Valencia, et al., The CD28-Transmembrane Domain Mediates Chimeric Antigen Receptor Heterodimerization With CD28, Front Immunol. 12 (2021) 639818, https://doi.org/10.3389/fimmu.2021.639818.
[15] A. Ershova, A. Goldaeva, A. Staliarova, E. Bulatov, A. Petukhov, N. Barlev, Future perspectives on novel CAR-T therapeutics beyond CD19 and BCMA in onco-hematology, Front Immunol. 16 (2025) 1592377, https://doi.org/10.3389/fimmu.2025.1592377.
[16] N. Watanabe, P. Bajgain, S. Sukumaran, S. Ansari, H.E. Heslop, C.M. Rooney, et al., Fine-tuning the CAR spacer improves T-cell potency, Oncoimmunology 5 (12) (2016) e1253656, https://doi.org/10.1080/2162402X.2016.1253656.
[17] A. Teplyakov, Y. Zhao, T.J. Malia, G. Obmolova, G.L. Gilliland, IgG2 Fc structure and the dynamic features of the IgG CH2-CH3 interface, Mol. Immunol. 56 (1-2) (2013) 131–139, https://doi.org/10.1016/j.molimm.2013.03.018.
[18] A. Hombach, A.A. Hombach, H. Abken, Adoptive immunotherapy with genetically engineered T cells: modification of the IgG1 Fc 'spacer' domain in the extracellular moiety of chimeric antigen receptors avoids 'off-target' activation and unintended initiation of an innate immune response, Gene Ther. 17 (10) (2010) 1206–1213, https://doi.org/10.1038/gt.2010.91.
[19] M.H. Dos Santos, M.P. Machado, P.R. Kumaresan, T.A. da Silva, Modification of Hinge/Transmembrane and Signal Transduction Domains Improves the Expression and Signaling Threshold of GXMR-CAR Specific to Cryptococcus spp, Cells 11 (21) (2022), https://doi.org/10.3390/cells11213386.
[20] L. Alabanza, M. Pegues, C. Geldres, V. Shi, J.J.W. Wiltzius, S.A. Sievers, et al., Function of Novel Anti-CD19 Chimeric Antigen Receptors with Human Variable Regions Is Affected by Hinge and Transmembrane Domains, Mol. Ther. 25 (11) (2017) 2452–2465, https://doi.org/10.1016/j.ymthe.2017.07.013.
[21] R.G. Majzner, S.P. Rietberg, E. Sotillo, R. Dong, V.T. Vachharajani, L. Labanieh, et al., Tuning the antigen density requirement for CAR T-cell activity, Cancer Discov. 10 (5) (2020) 702–723.
[22] D. Wang, R. Starr, D. Alizadeh, X. Yang, S.J. Forman, C.E. Brown, Vitro Tumor Cell Rechallenge For Predictive Evaluation of Chimeric Antigen Receptor T Cell Antitumor Function, 10.3791/, J. Vis. Exp. (144) (2019) 59275, https://doi.org/10.3791/59275.
[23] F. Yang, R. Liu, K.X. Hu, Exploring the mechanisms of CD19 CAR T-cell failure and salvage strategies in B-cell lymphoma, Hematol. Oncol. Discov. 1 (1) (2022) 44–54.
[24] M.Y. Balkhi, G. Wittmann, F. Xiong, R.P. Junghans, YY1 Upregulates Checkpoint Receptors and Downregulates Type I Cytokines in Exhausted, Chronically Stimulated Human T Cells, iScience 2 (2018) 105–122, https://doi.org/10.1016/j.isci.2018.03.009.
[25] H. Kinoshita, C.M. Bollard, K. Toner, editors. CD19 CAR-T cell therapy for relapsed or refractory diffuse large B cell lymphoma: Why does it fail?. Seminars in hematology Elsevier, 2023.
[26] M.H. Townsend, Z.E. Ence, T.P. Cox, J.E. Lattin, W. Burrup, M.K. Boyer, et al., Evaluation of the upregulation and surface expression of hypoxanthine guanine phosphoribosyltransferase in acute lymphoblastic leukemia and Burkitt's B cell lymphoma, Cancer Cell Int 20 (2020) 375, https://doi.org/10.1186/s12935-020-01457-8.
[27] M. Hamieh, A. Dobrin, A. Cabriolu, S.J.C. van der Stegen, T. Giavridis, J. Mansilla-Soto, et al., CAR T cell trogocytosis and cooperative killing regulate tumour antigen escape, Nature 568 (7750) (2019) 112–116, https://doi.org/10.1038/s41586-019-1054-1.
[28] R.S.O.C. Kawalekar OU, J.A. Fraietta, L. Guo, S.E. McGettigan, A.D. Posey Jr., et al., Distinct Signaling of Coreceptors Regulates Specific Metabolism Pathways and Impacts Memory Development in CAR T Cells, Immunity 44 (3) (2016) 712, https://doi.org/10.1016/j.immuni.2016.02.023.
[29] G.J. van der Windt, B. Everts, C.H. Chang, J.D. Curtis, T.C. Freitas, E. Amiel, et al., Mitochondrial respiratory capacity is a critical regulator of CD8+ T cell memory development, Immunity 36 (1) (2012) 68–78, https://doi.org/10.1016/j.immuni.2011.12.007.
[30] Z. Zhang, D. Huang, J. Feng, W. Li, Z. Wang, M. Lu, et al., PDE5 inhibitors against cancer via mediating immune cells in tumor microenvironment: AI-based approach for future drug repurposing exploration, Interdiscip. Med. 2 (3) (2024) e20230062.
[31] D. Ryan, C. Frezza, IL-10-Mediated Refueling of Exhausted T Cell Mitochondria Boosts Anti-Tumour Immunity, Immunometabolism 3 (4) (2021) e210030, https://doi.org/10.20900/immunometab20210030.
[32] Y. Zhao, J. Chen, M. Andreatta, B. Feng, Y.Q. Xie, M. Wenes, et al., IL-10-expressing CAR T cells resist dysfunction and mediate durable clearance of solid tumors and metastases, Nat. Biotechnol. 42 (11) (2024) 1693–1704, https://doi.org/10.1038/s41587-023-02060-8.
[33] H. Kinoshita, C.M. Bollard, K. Toner, CD19 CAR-T cell therapy for relapsed or refractory diffuse large B cell lymphoma: Why does it fail? Semin Hematol. 60 (5) (2023) 329–337, https://doi.org/10.1053/j.seminhematol.2023.11.007.
[34] S. Xie, J. Long, R. Wang, R. Xiang, H. Xian, Y. Wang, et al., Improved CAR internalization and recycling through transmembrane domain optimization reduces CAR-T cytokine release and exhaustion, Front Immunol. 16 (2025) 1531344, https://doi.org/10.3389/fimmu.2025.1531344.